

IAC-18.C4.6.4x46387

## Advances on the Inductive Plasma Thruster Design for an Atmosphere-Breathing EP System

Francesco Romano<sup>d\*</sup>, Georg H. Herdrich<sup>d</sup>, Adam Boxberger<sup>d</sup>, Peter C.E. Roberts<sup>a</sup>, Silvia Rodriguez-Donaire<sup>e</sup>, Daniel Garcia-Almiñana<sup>c</sup>, Miquel Sureda<sup>c</sup>, Nicholas H. Crisp<sup>a</sup>, Steve Edmondson<sup>a</sup>, Sarah Haigh<sup>a</sup>, Rachel E. Lyons<sup>a</sup>, Vitor T.A. Oiko<sup>a</sup>, Katharine Smith<sup>a</sup>, Sabrina Livadiotti<sup>a</sup>, Jonathan Becedas<sup>b</sup>, Gerardo González<sup>b</sup>, Rosa M. Dominguez<sup>b</sup>, Leonardo Ghizoni<sup>c</sup>, Victor Jungnell<sup>c</sup>, Kristian Bay<sup>c</sup>, Jonas Morsbøl<sup>c</sup>, Tilman Binder<sup>d</sup>, Constantin Traub<sup>d</sup>, Stefanos Fasoulas<sup>d</sup>, Dhiren Kataria<sup>f</sup>, Ron Outlaw<sup>g</sup>, Rachel Villain<sup>h</sup>, Jose Santiago Perez<sup>h</sup>, Alexis Conte<sup>h</sup>, Badia Belkouchi<sup>h</sup>, Barbara Heißerer<sup>i</sup>, Ameli Schwalber<sup>i</sup>

<sup>a</sup> The University of Manchester, *Oxford Road, Manchester, M13 9PL, United Kingdom*

<sup>b</sup> Elecnor Deimos Satellite Systems, *C/ Francia 9, 13500 Puertollano, Spain*

<sup>c</sup> GomSpace AS, *Alfred Nobels Vej. 21A, 9220 Aalborg East, Denmark*

<sup>d</sup> Institute of Space Systems (IRS), University of Stuttgart, *Pfaffenwaldring 29, 70569 Stuttgart, Germany,*

\*Corresponding author: [romano@irs.uni-stuttgart.de](mailto:romano@irs.uni-stuttgart.de)

<sup>e</sup> UPC-BarcelonaTECH, *Colom 11, TR5 08222 Terrassa, Barcelona, Spain*

<sup>f</sup> Mullard Space Science Laboratory (UCL), *Holmbury St. Mary, Dorking, Surrey, RH5 6NT, United Kingdom*

<sup>g</sup> Christopher Newport University, *Newport News, Virginia 23606, US*

<sup>h</sup> Euroconsult, *86 Boulevard de Sébastopol, 75003 Paris, France*

<sup>i</sup> Concentris Research Management GmbH, *Ludwigstraße 4, D-82256 Fürstentfeldbruck, Germany*

### Abstract

Challenging space mission scenarios include those in very low Earth orbits, where the atmosphere creates significant drag to the S/C and forces their orbit to an early decay. For drag compensation, propulsion systems are needed, requiring propellant to be carried on-board. An atmosphere-breathing electric propulsion system (ABEP) ingests the residual atmosphere through an intake and uses it as propellant for an electric thruster. Theoretically applicable to any planet with atmosphere, the system might allow drag compensation for an unlimited time without carrying propellant. A new range of altitudes for continuous operation would become accessible, enabling new scientific missions while reducing the required effort for the launcher by achieving these low orbits. Preliminary studies have shown that the collectible propellant flow for an ion thruster in low Earth orbit (LEO) might not be enough, and that electrode erosion due to aggressive gases, such as atomic oxygen, will limit the thruster's lifetime. In this paper we present the advances on the design of an inductive plasma thruster (IPT) for the ABEP. The IPT is based on a small-scale inductively heated plasma generator IPG6-S. IPG have the advantage of being electrodeless, and have already shown high electric-to-thermal coupling efficiencies using O<sub>2</sub> and CO<sub>2</sub> as propellant. IPG6-S requires a scaling of the discharge channel to meet with power requirement and expected collected mass flows, as well as optimisation of the accelerating stage, to provide the required thrust to the spacecraft. Tests have been performed to verify some of the parameters and are as well presented within this paper.

**Keywords:** ABEP, IPG, IPT, VLEO, RAM-EP

### Acronyms/Abbreviations

ABEP: Atmosphere-Breathing Electric Propulsion  
IPT: Inductive Plasma Thruster

IPG: Inductively heated Plasma Generator

VLEO: Very Low Earth Orbit

S/C: Spacecraft

### 1. Introduction

Missions in very-low Earth orbit (VLEO) may open new opportunities for scientific and civil use, such as geomagnetic field measurements, weather forecasting, oceanic currents monitoring, polar ice caps, fires, agriculture, and surveillance services. ESA mission GOCE has ended in 2013, by orbiting as low as 229 km, it provided detailed information of Earth's geomagnetic field using gridded ion thrusters (GIT) to

compensate the drag [1]. Aerodynamic drag at such low altitudes limits the mission lifetime. This drag needs to be compensated by an efficient propulsion system. In VLEO simpler and smaller platforms are possible. Moreover, the drag also provides self de-orbiting at the end of the mission [2]. For such missions, the maximum mission lifetime of a S/C is a mission design driver that depends on the amount of drag that

the propulsion system can compensate, and for how long. Within the EU-funded H2020 DISCOVERER project, key technologies for VLEO orbiting platforms are being developed. In particular, IRS has the task of develop and test an Atmosphere-Breathing Electric Propulsion system (ABEP) that could enable such platforms. Such propulsion system technology utilizes an intake to collect the residual atmosphere in VLEO, and use it as propellant for an inductive plasma thruster (IPT). In the framework of the H2020 project, the market constraints are being analysed in order to place ABEP as a feasible technology in future VLEO missions. Extending the lifetime of any mission is the major benefit to improve their associated incomes. In summary, the pros and cons of ABEP, from a market point of view are being modelled in order to get clear inputs for the new stakeholders in the VLEO field.

## 2. Atmosphere-Breathing Electric Propulsion

In an Atmosphere-Breathing Electric Propulsion (ABEP) system, an intake collects the residual atmosphere of a planet, and feeds an electric thruster. This uses it as propellant to produce a thrust capable of compensating the drag. In this particular case an inductive plasma thruster is used, see Figure 1.

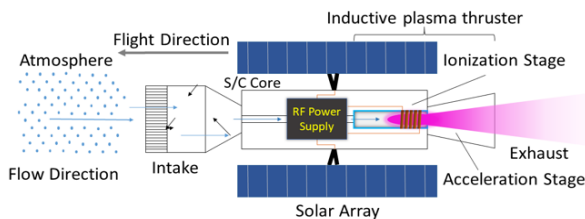


Figure 1 ABEP Principle of operation [2]

An IPT is based on IPG technology developed at IRS. RF-current is fed to a coil/antenna that is wrapped around a discharge channel made of quartz. Within the discharge chamber the propellant (gas) is flowing. Time-varying electric and magnetic fields produced through the coil, ionize the gas inside the discharge channel and transform it into plasma, see Figure 2.

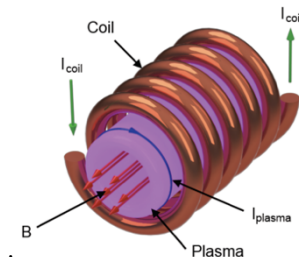


Figure 2 IPG Principle of operation [3]

The process is done without electrodes, therefore no component has direct contact with the plasma, leading

to the advantage of very high propellant flexibility and completely removes the issue of electrode erosion. This last phenomena leads to performance degradation over time with common electric propulsion technologies, such as RIT and HET, especially when aggressive gases, such as atomic oxygen, are used [4], [5].

## 3. Candidate IPT for ABEP application

Extended testing has been performed by operating the inductively heated plasma generator IPG6-S with CO<sub>2</sub>, N<sub>2</sub>, and O<sub>2</sub>, and mixtures according to an ABEP-based system analysis [6]–[8]. IPG6-S is not optimized to run on atmospheric propellant and it is not designed for propulsion purposes. However, it serves to evaluate plasma discharges with atmospheric propellants, and mass flows according to the system analysis deriving from intake performance estimation through simulations [9]. Results have shown that an optimisation of the plasma source for the given mass flow is required and, that high exhaust velocity are necessary to provide enough thrust for drag compensation purposes [7], [8]. In order to reach such high exhaust velocities, electromagnetic acceleration is necessary. For the electromagnetic acceleration to be as effective as possible, a degree of ionization as close as possible to full, is required. Therefore, the first step for the development of an IPT for ABEP application, is the production of a high degree of ionization plasma. According to [10]–[15] higher density plasma ( $n > 10^{18} \text{ m}^{-3}$ ) can be produced at lower power, compared to ICP, if a DC magnetic field is applied to the discharge. Therefore, simulation tools have been used to perform the design of a new plasma source, optimized for ABEP-application.

The first simulation tool used has been HELIC, developed by Arnush and Chen [12]. The parameters of IPG6-S have been applied to verify the improvement of the generator by applying an externally applied DC magnetic field. Second, most of the parameters have been varied to develop the new plasma source for the future IPT, details of this work can be seen in [16].

## 4. IPT Design

According to simulation results, the use of high frequency together with an externally applied DC magnetic field, higher plasma coupling efficiency can be achieved by an increase of plasma resistance for ABEP-related estimated gas densities [7], [8].

Leaded by the simulation results, an RF-Generator and an auto-matching network that provides power input up to 4 kW has been acquired. The first design of the IPT, started with a quartz tube diameter of 40 mm, the

same as that of IPG6-S, with a design aimed to maximum flexibility. This last requirement ruled out the use of water cooling, except for the inside of the antenna/coil. The maximum flexibility is achieved by the possibility of easy change of coil/antenna, number of turns, cross section, shape, and its position along the quartz tube. The gas injection system has been designed so that an injector with different swirl angles can be used, and its position along the discharge channel easily changed, so to increase and decrease the discharge channel length. An electromagnet, described in the next section, is installed. The magnetic field intensity can be changed by varying the applied current, and it can also be moved along the discharge channel. The plasma source is mounted outside the vacuum chamber, see Figure 3.

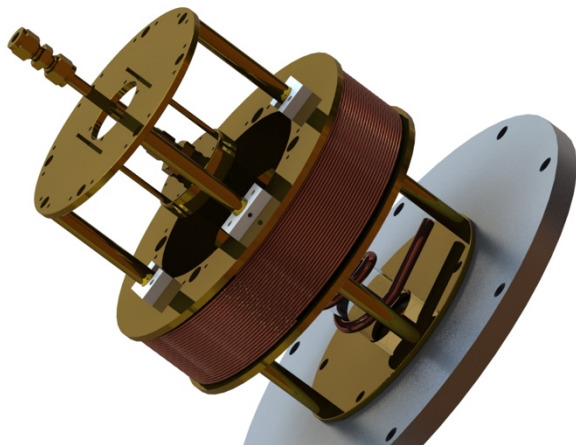


Figure 3 IPT Assembly Rendering

### 5. Electromagnet design

To verify the simulation results in [16], an electromagnet has been built to produce the required magnetic field. Instead of relying on permanent magnets, flexibility in terms of magnetic field strength has been chosen. The electromagnet has been designed to fit both IPG6-S and IPT, a common electromagnet design has been achieved, so that one device could serve both facilities in the required magnetic field range. First set of simulations, see [7], [8], have shown that a DC magnetic field between 20 and 60 mT is required to efficiently increase the plasma coupling efficiency [16]. The design requirements for the electromagnet have been:

- Magnetic field strength > 60 mT;
- Size (fit to both IPG6-S and IPT);
- Available DC power supply, maximum current 15 A;
- Minimum 30 minutes of steady state operation ( $T < 200^{\circ}\text{C}$ );
- No water cooling.

Given the requirements, a magnetic wire of 2 mm diameter has been selected, with an insulation that can achieve a maximum operating temperature of  $200^{\circ}\text{C}$ . The final magnetic wire length is of  $\sim 600$  m, and with  $\sim 800$  turns, capable of generating a magnetic field > 60 mT with the given maximum 15 A.

Before the operation with the plasma source, the magnetic field intensity has been measured for different currents by means of a Teslometer positioned along the axis of the electromagnet, the results are shown in Figure 4.

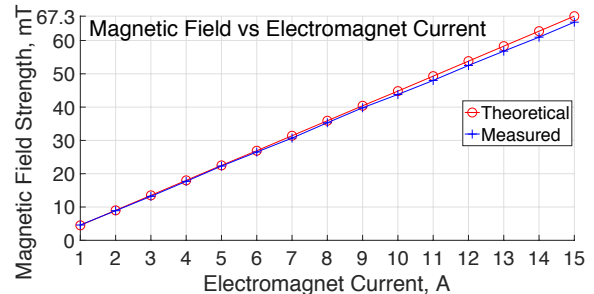


Figure 4 Electromagnet Performance, measured and theoretical.

### 6. Facility Set-Up Description

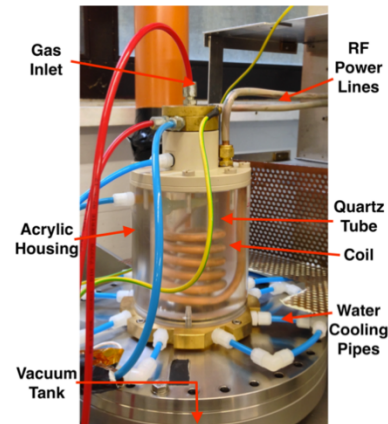


Figure 5 IPG6-S (EM not installed)

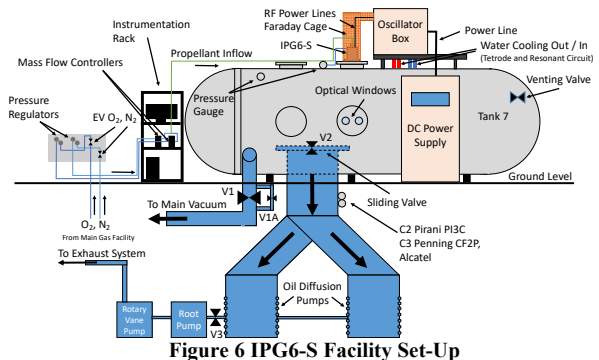


Figure 6 IPG6-S Facility Set-Up

IPG6-S, see Figure 5, is composed by a discharge channel made of quartz with an internal diameter of 37 mm, and a length of 180 mm. A 5.5-turn internally water cooled copper coil is wrapped around the discharge channel. The top injector head, the bottom flange, and the de Laval nozzle are made of brass, all water cooled. The IPG6-S housing is made of acrylic and holds together the structure. The de Laval nozzle has a modular design [8] and is currently with a throat diameter of 20 mm, and an outlet diameter of 40 mm. The facility at its whole is depicted in Figure 6. The vacuum chamber, has a cylindrical shape with a length of 4.8m and a diameter of 2 m. The main vacuum facility at IRS provides a total pumping speed of more than 250 000 m<sup>3</sup>/h. IPG6-S is mounted on a flange on the top of the vacuum chamber directing the plasma downwards. With the main vacuum system, a base pressure of < 0.3 Pa is achieved with no gas flow.

The electrical power is provided by the RF generator Himmelwerk HGL 20-4B, with a maximum of 20 kW power at a frequency of ~ 4 MHz, dependent on the impedance of IPG6-S. It is composed of two main elements: the high voltage DC power supply, air-cooled, located on the side of the vacuum chamber, and the oscillator that produces the RF signal for IPG6-S, located on the top of the vacuum chamber close to IPG6-S. The oscillator is provided with a tetrode and the resonant circuit that includes the IPG6-S coil, both of them are water cooled. The high voltage DC power provides a high voltage of 7.7, 8.2, 8.5 kV, that directly feeds the tetrode in the oscillator. In parallel a voltage between -150 and 200 V is delivered to the triode in the power supply, the latter serves to produce the DC voltage from 0 to 1.7 kV that regulates the screen grid of the tetrode in the oscillator. The higher the applied screen grid voltage is, the larger is the current allowed to flow through the tetrode, with a maximum of  $I_A = 4$  A. The output current flows through the resonant circuit that determines, together with the IPG6-S coil, the operating frequency, in the current configuration at 3.3 MHz. The active power  $P_{RF}$  that is finally delivered, is the regulated value of the power supply.

## 7. Electromagnet Testing

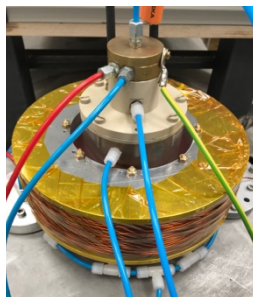


Figure 7 IPG6-S with EM installed

The electromagnet (EM) applied to IPG6-S has been applied in the last second half of September 2018, therefore only preliminary results are hereby shown. The EM has been installed at the height of the coil, see Figure 6. Tests have been performed with N<sub>2</sub>, O<sub>2</sub>, and Ar as propellant, at mass

flows rates < 10 mg/s, corresponding to injector pressures < 15 Pa. Tank pressure has been always between 0.2 - 0.7 Pa with gas flow active. At the lowest mass flows, ignition could not be achieved without the aid of the EM. Oscillations in the active power signal, and RF coil current and voltage profile on the oscilloscope are visible. During testing, it has been observed that these oscillations can be reduced by varying the magnetic field. The reduction of oscillations in the signals can be read as a reduction of the reflected power by the plasma to the power supply. The test procedure was to first find the plasma ignition point without aid of externally applied magnetic field. If the ignition was not achieved, the EM was turned on when the anode current was between 1.8 - 2 A, and the magnetic field intensity gradually increased. In most cases, 5 mT have been enough to trigger plasma ignition. Second, the RF power was increased up to the facility maximum, corresponding to 4 A anode current. There, a further increase of magnetic field was applied: this produced a steep increase of RF active power for a factor greater than 2 as can be seen in the results section. This first test served to estimate the effect of magnetic field on the ignition point, and its possibility to aid the absorbed power by changing plasma properties.

## 8. Results

In Figure 8, Figure 9, and Figure 10, results for N<sub>2</sub>, O<sub>2</sub>, Ar as operating gases for IPG6-S are presented. These are representing the power absorbed by the plasma, and the anode current of the power supply. The injector pressure, corresponding to the pressure inside the discharge chamber is also shown, together with the cooling power of the same discharge chamber, estimated by the cooling water temperature difference. On top of the plots, the ignition point is highlighted. Since there is no integration yet with the EM power supply and our data acquisition system, the magnetic field strength is showed on the plot directly. The signal of the  $P_{RF}$  is a combination of the signals of RF current and voltage at the coil. The ignition point shows a high  $P_{RF}$  that is not yet coupled into the plasma that shows a sudden drop to a more stable signal, this corresponds to plasma ignition. For the N<sub>2</sub> test, ignition could be easily achieved without aid of EM, while O<sub>2</sub> and Ar required so. Applying 5.4 mT could already increase double  $P_{RF}$ , while 18.2 mT could to 2800 W, however, with high reflection. A noticeable increase of  $P_{RF}$  could be achieved by increasing  $I_A$  to 4.2 A (above the power supply limit), suggesting that higher currents are required for the plasma source. The O<sub>2</sub> test, shows a much lower signal oscillation, corresponding to a better matching power and more continuous power delivery to the plasma. An applied magnetic field of



27.1 mT could increase the absorbed power from 500 W to 3700 W. The Ar test, shows an higher required magnetic field strength to provide the ignition, now 11.3 mT, and the amplification of  $P_{RF}$ . This is due to the Ar properties, and the influence of the low pressure in the discharge chamber, around 5 Pa, compared to the  $O_2$  and  $N_2$  tests. Moreover, an increase of  $I_A$  from 2.5 A to 3 A caused the plasma to switch off, while the power supply remain operational. This point requires further investigation. Moreover, in all tests, a saturation in terms of magnetic field is reached at different intensities, this agrees to the study of [17].

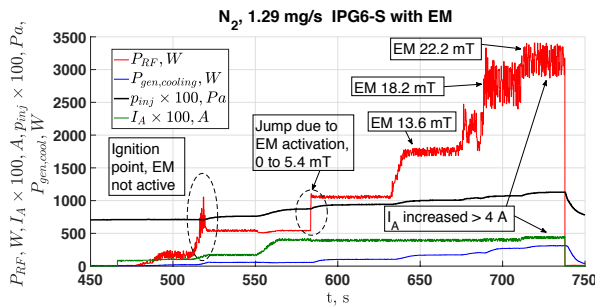


Figure 8  $N_2$  Test, effect of applied magnetic field

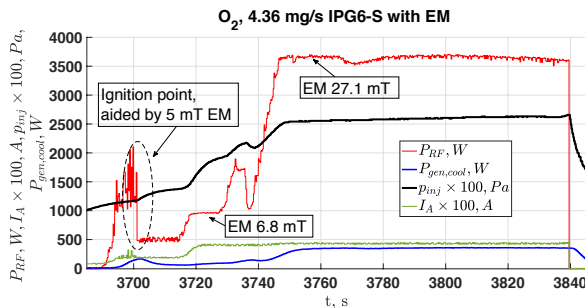


Figure 9  $O_2$  Test, effect of applied magnetic field

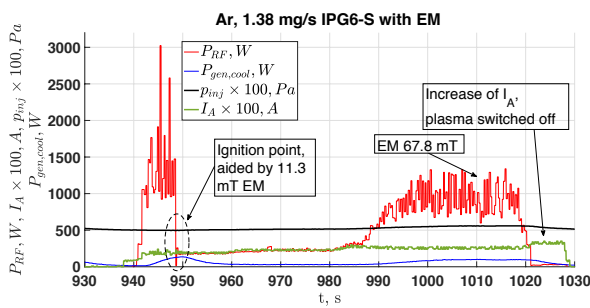


Figure 10 Ar Test, effect of applied magnetic field

## 9. Conclusions and Outlook

The influence of externally applied magnetic field has been analysed based on simulations performed with HELIC tool based on previous studies [16]. These have shown that an increase of plasma resistance could be achieved if an externally magnetic field is applied. An electromagnet has been built and put into

operation, designed to work with both IPG6-S and the upcoming IPT.

Parallely, the IPT has been designed and almost completely assembled. The implementation into its facility is to be done within the next months, expecting ignition in early 2019. The tank 12 facility will be equipped with plasma diagnostics such as retarding potential analyser (RPA), Langmuir and Farady probe, optical emission spectroscopy (OES), laser induced fluorescence (LIF), tunable diode laser absorption spectroscopy (TDLAS). These tools are fundamental to measure plasma characteristics.

Preliminary testing of the EM has been conducted with IPG6-S. The application of the magnetic field has shown three advantages:

- Plasma ignition is aided by B-field;
- Power reflection is reduced by B-field;
- Power absorbed is amplified by B-field.

Such effects show that an improvement for the plasma source are achieved by applying a magnetic field. Such results are promising especially for an ABEP application. As there are variation on incoming mass flow and propellant composition, the point of operation must be adjusted, and this can be achieved by a variation of the magnetic field only, such to control the plasma resistance and, therefore, the power absorbed and, finally the thrust.

These test results will be analysed in detail and compared with HELIC results, but also with more advanced simulation tools. A comparison of different gases with same  $p_{inj}$  are planned. The conclusion of these comparisons will aid to the design for the upcoming IPT.

## 10. Acknowledgements

This project has received funding from the European Union's Horizon 2020 research and innovation programme under grant agreement No. 737183. This reflects only the author's view and the European Commission is not responsible for any use that may be made of the information it contains. Special big thanks for the support to Yung-An Chan, Nicholas Harmansa, Adam Pagan, Silvia Masillo, and Ruggero Soglia.

## Bibliography

- [1] Alenia Spazio, "Goce Gravity field and steady-state Ocean Circulation Explorer," System Critical Design Review, 2005.
- [2] F. Romano, B. Massuti-Ballester, T. Binder, G. Herdrich, S. Fasoulas, and T. Schönherr, "System analysis and test-bed for an

- atmosphere-breathing electric propulsion system using an inductive plasma thruster,” *Acta Astronaut.*, vol. 147, pp. 114–126, 2018.
- [3] G. Herdrich, “Aufbau, Qualifikation und Charakterisierung einer induktiv beheizten Plasmawindkanalanlage zur Simulation atmosphärischer Eintrittsmanöver.”
- [4] G. Cifali, T. Misuri, P. Rossetti, M. Andrenucci, D. Valentian, D. Feili, and B. Lotz, “Experimental characterization of HET and RIT with atmospheric propellants,” in *International Electric Propulsion Conference*, 2011, pp. 1–12.
- [5] G. Cifali, D. Dignani, T. Misuri, P. Rossetti, D. Valentian, F. Marchandise, D. Feili, and B. Lotz, “Completion of HET and RIT characterization with atmospheric propellants,” in *Space Propulsion 2012 2355386*, 2012, no. May, pp. 7–10.
- [6] F. Romano, B. Massuti-Ballester, T. Schönherr, and G. Herdrich, “System Analysis and Test Bed for an Air-Breathing Electric Propulsion System,” in *5th Russian-German Conference on Electric Propulsion (RGCEP), Dresden, Germany, 2014*.
- [7] Romano et al, “System Analysis and Test-Bed for an Atmosphere-Breathing Electric Propulsion System Using an Inductive Plasma Thruster,” *67th Int. Astronaut. Congr.*, no. September, pp. 25–29, 2017.
- [8] F. Romano, G. Herdrich, and S. Fasoulas, “Performance Evaluation of a Novel Inductive Atmosphere-Breathing EP system,” in *International Electric Propulsion Conference*, 2017, no. October, pp. 1–2.
- [9] F. Romano, T. Binder, G. Herdrich, F. S, and T. Schönherr, “Air-Intake Design Investigation for an Air-Breathing Electric Propulsion System,” *34th Int. Electr. Propuls. Conf. Kobe, Japan.*, 2015.
- [10] F. F. Chen and R. W. Boswell, “Helicons-the past decade,” *IEEE Trans. Plasma Sci.*, vol. 25, no. 6, pp. 1245–1257, 1997.
- [11] F. F. Chen, “Physics of helicon discharges,” *Phys. Plasmas*, vol. 3, no. 5, p. 1783, 1996.
- [12] F. F. Chen and D. Arnush, “Generalized theory of helicon waves. I. Normal modes,” *Phys. Plasmas*, vol. 4, no. 9, p. 3411, 1997.
- [13] D. Arnush and F. F. Chen, “Generalized theory of helicon waves. II. Excitation and absorption,” *Phys. Plasmas*, vol. 5, no. 5, p. 1239, 1998.
- [14] F. F. Chen, “Permanent magnet Helicon source for ion propulsion,” *IEEE Trans. Plasma Sci.*, vol. 36, no. 5 PART 1, pp. 2095–2110, 2008.
- [15] F. F. Chen and H. Torreblanca, “Permanent-magnet helicon sources and arrays: A new type of rf plasma,” *Phys. Plasmas*, vol. 16, no. 5, pp. 1–8, 2009.
- [16] F. Romano, G. Herdrich, T. Binder, A. Boxberger, C. Traub, S. Fasoulas, T. Schönherr, P. Roberts, K. Smith, S. Edmondson, S. Haigh, N. Crisp, V. T. A. Oiko, R. Lyons, S. D. Worrall, S. Livadiotti, J. Becedas, G. Gonzalez, R. M. Dominguez, L. Ghizoni, V. Jungnell, K. Bay, J. Morsbøl, D. Garcia-Almiñana, S. Rodriguez-Donaire, M. Sureda, D. Kataria, R. Outlaw, R. Villain, J. S. Perez, A. Conte, B. Belkouchi, A. Schwalber, and B. HeiBerer, “Effects of applied magnetic field on IPG6-S , test-bed for an ABEP-based inductive plasma thruster (IPT),” *Sp. Propuls. 2018*, no. 1, 2018.
- [17] E. A. Kralkina, A. A. Rukhadze, P. A. Nekliudova, V. B. Pavlov, A. K. Petrov, and K. V. Vavilin, “RF power absorption by plasma of low pressure low power inductive discharge located in the external magnetic field,” *AIP Adv.*, vol. 8, no. 3, 2018.